Molecular Nutrition & Food Research
www.mnf-journal.com

Physiologically-Based Kinetic Modeling Predicts Similar In Vivo Relative Potency of Senecionine N-Oxide for Rat and Human at Realistic Low Exposure Levels

Frances Widjaja, Yasser Alhejji, Jamyang Yangchen, Sebastiaan Wesseling, and Ivonne M. C. M. Rietjens*

Scope: This study aims to determine if previously developed physiologically-based kinetic (PBK) model in rat can be modified for senecionine (SEN) and its N-oxide (SENO), and be used to investigate potential species differences between rat and human in relative potency (REP) of the N-oxide relative to the parent pyrrolizidine alkaloid (PA).

Methods and results: In vitro derived kinetic parameters including the apparent maximum velocities (V_{max}) and Michaelis–Menten constants (K_m) for SENO reduction and SEN clearance are used to define the PBK models. The rat model is validated with published animal data, and the toxicokinetic profiles of SEN from either orally-administered SENO or SEN are simulated. REP values of SENO relative to SEN amount to 0.84 and 0.89 in rat and human, respectively.

Conclusion: The REP value can be dose- and species-dependent, with the values for rat and human being comparable at low realistic exposure scenarios. In summary, PBK modeling serves as a valuable New Approach Methodology (NAM) tool for predicting REP values of PA-N-oxides and may actually result in more accurate REP values for human risk assessment than what would be defined using in vivo animal experiments.

1. Introduction

Pyrrolizidine alkaloids (PAs) are secondary plant metabolites found in 3% of flowering plants[1–3] and in food commodities such as honey, tea, plant food supplements, herbs, and spices.[4] Humans are exposed to PAs via two main pathways, namely accidental contamination of foodstuffs and deliberate use of PA-containing plants in herb based foodstuffs.[5] For example, chronic foodstuff contamination in South Africa from *Senecio* and *Crotalaria* make their way into grains that are used to prepare food, and *Senecio* extracts are also used to prepare tea as remedy for medical conditions such as amenorrhea and menorrhagia.[6] *Senecio* plants are known to contain senecionine (SEN) and its N-oxide (SENO)[7–10] and *Senecio* poisoning has been reported to cause liver carcinoma.[6] Recent studies show that consumption of *Gynura segetum* herbal samples containing high levels of SENO also caused acute toxicity in the form of the hepatic sinusoidal obstruction syndrome.[11]

More than 660 different structures of PAs and their N-oxides (PA-N-oxides) have been identified.[12] In plants, PAs coexist with their N-oxides[13,14] with PA-N-oxides being identified as the dominant form.[7,15] PA-N-oxides must first be reduced to their parent PAs before causing toxicity (**Figure 1**).[11,16–21] This reduction primarily takes place in two body compartments: the large intestine where conversion occurs by intestinal microbiota and the liver.[16–18] PAs are detoxified through N-glucuronidation,[22] hydrolysis,[15,23] or N-oxidation to their N-oxides,[24] while reduction of the N-oxides regenerates the PAs. PAs with an 1,2-unsaturated bond are protoxins that can be metabolically oxidized into bioactive pyrroles such as dehydropyrrolizidine alkaloids (DHPAs) and subsequently hydrolyzed into (±)-6,7-dihydro-7-hydroxy-1-hydroxymethyl-5H-pyrrolizine (DHP).[21] These pyrrole moieties can react with glutathione (GSH)[25] or form covalent bonds[26] with protein or DNA leading to toxic pyrrole-protein adducts[27] and pyrrole-DNA adducts.[28] Upon reaction with GSH, the pyrrole moieties can still react with DNA as shown for instance for 7-GS-DHP, 7-cysteine-DHP, and 7-valine-DHP.[29] The protein and DNA pyrrole adducts

F. Widjaja, Y. Alhejji, J. Yangchen, S. Wesseling, I. M. C. M. Rietjens
Division of Toxicology
Wageningen University
PO Box 8000, Wageningen 6700 EA, The Netherlands
E-mail: frances1.widjaja@wur.nl
Y. Alhejji
Department of Food Science and Human Nutrition
College of Agriculture and Veterinary Medicine
Qassim University
Buraydah 51452, Saudi Arabia
J. Yangchen
Bhutan Agriculture and Food Regulatory Authority
Ministry of Agriculture and Forests
Thimphu 11002, Bhutan

The ORCID identification number(s) for the author(s) of this article can be found under https://doi.org/10.1002/mnfr.202200293

DOI: 10.1002/mnfr.202200293

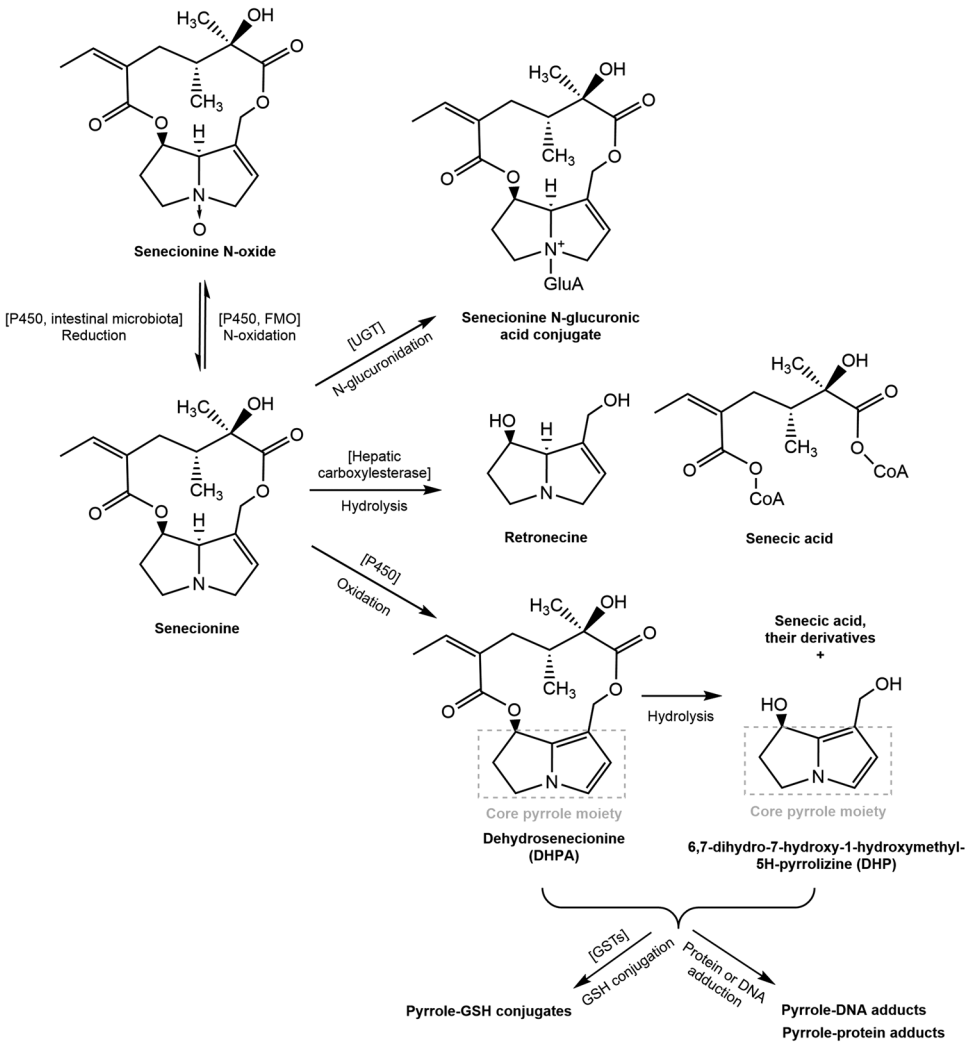

Figure 1. Metabolic pathway of SENO and SEN as adapted from He et al.[21]

subsequently cause hepatotoxicity,[21] genotoxicity,[22] and carcinogenicity.[23]

Given that exposure to PAs generally includes a mixture of PAs with different potency, definition of so-called relative potency (REP) values is essential for a combined risk assessment. However, given the large number of PAs and PA-N-oxides, it is unrealistic to determine these REP values by in vivo toxicity studies indicating the need for use of New Approach Methodologies (NAMs). In a previous study, we used physiologically based kinetic (PBK) modeling to show that REP values for PA-N-oxides are likely to be lower than those of their parent PAs.[30–32] This NAM was based on physiologically based kinetic (PBK) modeling and was able to take the reduction of the PA-N-oxide by the intestinal microbiota to the corresponding parent PA into account, a factor often ignored in in vitro model systems applied thus far to define REP values for PA-N-oxides.[30,31] This previous study also revealed the REP value for the riddelliine N-oxide (RIDO) to be dose-dependent with the REP value being lower at high dose levels used in animal experiments and higher at lower realistic dietary intake levels.[16] At these low dose levels, experimental quantification of the REP value becomes hampered by the detection limits of the experimental method applied, illustrating an important advantage of the PBK modeling based NAM. At dose levels realistic for human exposure, the REP value of RIDO relative to riddelliine (RID) amounted to 0.78, while at higher dose levels used in the available animal study, the REP value was 0.67. The PBK modeling also revealed that this decrease in the REP value with increasing dose level could be ascribed to saturation of the reduction of RIDO to RID when dosing RIDO and of the clearance of RID when dosing RID.

This study aims to use the previously validated PBK models for RID and RIDO in rats to develop PBK models for rats and humans for another PA, SEN, and its N-oxide, SENO, and to use the PBK models thus defined to investigate i) whether also for this PA-N-oxide the REP value is dose-dependent, and ii) whether the REP value is species-dependent. SENO and SEN were selected as the model compounds for the present study because they are among the 17 PAs in EFSA's list of PAs relevant for food and feed.[4] Another reason for the selection was that for SENO kinetic data from an in vivo rat study[11]

are available for PBK model evaluation. Given that different PAs show different kinetic profiles,[33] different PA-N-oxides might also demonstrate different kinetic profiles due to potential structure-dependent differences in reduction of the N-oxides to the parent PAs[20] and in metabolic clearance of the formed parent PAs.[34] Besides structure-dependent differences, there might also be species-dependent differences in the kinetics of PAs and their N-oxides potentially resulting in different REP values in rat and human. One species difference known to occur relates to the fact that in addition to being cleared by hepatic CYP450s and carboxylesterases, in humans PAs can additionally be cleared through N-glucuronidation by uridine 5′-diphospho-glucuronosyltransferase (UGT), a reaction not relevant in rats[22,35] (Figure 1).

2. Experimental Section

2.1. Materials and Standard Chemicals

SEN (98%) and SENO (91%) were purchased from Phytolab (Phytolab GmbH & Co. KG, Germany). Test chemicals were prepared in DMSO purchased from Acros Organics (Geel, Belgium). Acetonitrile (ACN) (UPLC/MS grade) and methanol were purchased from Biosolve (Valkenswaard, the Netherlands). Di-potassium hydrogen phosphate trihydrate ($K_2HPO_4 \cdot 3H_2O$) and potassium dihydrogen phosphate (KH_2PO_4) were purchased from Merck (Darmstadt, Germany). The reduced form of nicotinamide adenine dinucleotide phosphate (NADPH) was purchased from Carbosynth (Carbosynth, UK), while NADPH regeneration system was purchased from Tebu Bio B. V. (Heerhugowaard, the Netherlands). Phosphate-buffered saline (PBS, pH 7.4) was purchased from Gibco (Paisley, USA). Pooled rat and human liver S9 were purchased from Corning (Amsterdam, the Netherlands), and pooled rat small intestine S9 from Xenotech (Kansas City, USA). Fresh rat fecal samples from Wistar rats (10 males and 10 females) were a gift from BASF (Ludwigshafen, Germany) and were collected, treated, and stored as previously described.[16] Fresh human fecal samples (12 random donors) were obtained as previously described.[16,36] Both rat and human fecal samples were collected fresh immediately after feces excretion from donors. The rat fecal samples collection did not require ethical approval because they were given as gift from BASF, while the S9 fraction samples were purchased from industries that already possess the license to sell these materials for research purposes. The human fecal samples collection did not require ethical approval because METC Oost Nederland declare this study to not fall under the Act of Medical Research Involving Human Subjects (WMO), while the S9 fraction samples were purchased from industries that already possess the license to sell these materials for research purposes.

2.2. In Vitro Incubations with SENO and SEN to Derive Kinetic Parameters for the PBK Model

The kinetic constants (V_{max} and K_m) for SENO reduction to SEN were obtained from in vitro incubations of SENO with fecal material or liver S9 of rat or human, while the kinetic constants for SEN clearance were derived from in vitro incubations of SEN with liver S9 of both species. Under all incubation conditions (Table S1, Supporting Information), the conversion was linear with time and concentration of feces or S9[16,17,37–39] (data not shown). All measurements were performed in triplicate.

2.2.1. Anaerobic Rat and Human Fecal Incubations

Almost every study that incorporated in vitro incubations with fecal bacteria performed their experiments in a different manner. The aim of the present study was to obtain rate constants for microbial conversion by a microbial sample as closed to the intestinal microbial activity as possible, and therefore short incubations were performed using minimal medium (i.e., PBS) to prevent preferential growth of the microorganisms. This approach was also based on the fact that in previous studies this method appeared to provide kinetic constants able to adequately predict the in vivo kinetics.[36,37]

The incubation was performed in a total incubation volume of 100 µL containing anaerobic PBS, the amount of fecal slurry optimal for the incubation time (Table S1, Supporting Information), and 2–200 µM SENO (added from 50 times concentrated stock solution in DMSO). Controls were performed without the addition of fecal slurry. Samples were incubated in an anaerobic chamber (Sheldon, Cornelius, USA) at 37 °C under atmospheric conditions of 85% v/v N_2, 10% v/v CO_2, and 5% v/v H_2. Upon 5 min preincubation at 37 °C, the reaction was started by the addition of SENO. The reaction was terminated by adding one volume of ice-cold methanol followed by centrifugation at 21 500 x *g* for 15 min at 4 °C and supernatants were immediately analyzed with LC-MS/MS.

2.2.2. Aerobic Rat and Human S9 Incubations

The incubation was performed in a total volume of 100 µL containing (final concentrations) 0.1 M potassium phosphate (pH 7.4), 2 mM NADPH, the amount of liver S9 optimal for the incubation time (Table S1, Supporting Information), and 2–200 µM SENO (added from 50 times concentrated stock solution in DMSO). When reduction by liver S9 was done in an anaerobic setting, anaerobic phosphate buffer was used and the incubation was performed in an anaerobic environment as described for the fecal incubations. When the NADPH regeneration system was used, NADPH was replaced with NADPH regeneration system in the incubation. Controls were performed without the addition of NADPH or NADPH regeneration system. Upon 1 min preincubation with NADPH in a shaking water bath at 37 °C, the reaction was started by the addition of SENO. The reaction was terminated by adding 20% v/v ice-cold ACN followed by centrifugation at 16 000 × *g* for 5 min at 4 °C and supernatants were immediately analyzed with LC–MS/MS.

To measure SEN clearance, liver S9 was used because hepatic CYP450 and carboxylesterases are found in both the microsome and cytosol. The incubation was performed in a total volume of 100 µL containing (final concentrations) 0.1 M potassium phosphate (pH 7.4), 2 mM NADPH, the amount of liver S9 optimal for the incubation time (Table S1, Supporting Information), and

0.5–50 µM SEN (added from 20 times concentrated stock solution in DMSO). SEN was only prepared up to 1 mM due to solubility issues.[31] Controls were performed without the addition of NADPH. Upon 5 min preincubation with NADPH in a shaking water bath at 37 °C, the reaction was started by the addition of SEN. The reaction was terminated by the addition of 20% v/v ice-cold ACN followed by centrifugation at 16 000 x *g* for 5 min at 4°C and the supernatants were immediately analyzed with LC–MS/MS.

2.3. LC-MS/MS Analysis

SEN and SENO were quantified by LC–MS/MS[16,39] using a Shimadzu Nexera XR LC-20AD XR UHPLC System coupled with a Shimadzu LCMS-8045 MS (Kyoto, Japan). A 1 µL aliquot was loaded into a reverse phase C18 column (Phenomenex 1.7 µm 2.1 × 50 mm). The flow rate was 0.3 mL min^{-1} and the mobile phase was made with ultrapure water with 0.1% v/v formic acid and ACN containing 0.1% v/v formic acid. A linear gradient was applied from 0% to 100% ACN in 7 min. This percentage was kept for 1 min, after which it was reduced back to the starting conditions of 0% ACN in 1 min and the column was equilibrated for another 4 min at the starting conditions before the next injection. Under these conditions, SEN eluted at 4.2 min and SENO at 4.3 min. For detection a Shimadzu LCMS-8045 triple quadrupole with ESI interface was used. The instrument was operated in positive ionization mode in the multiple reaction monitoring (MRM) mode with a spray voltage of 4.0 kV. SENO was monitored at the $[M + H]^+$ of precursor to products of 352.1 → 94.20 (CE = −50 eV), 352.1 → 118.20 (CE = −38 eV) and 352.1 → 120.25 (CE = −39 eV). SEN was monitored at the $[M + H]^+$ of precursor to products of 336.1 → 94.10 (CE = −37 eV), 336.1 → 120.15 (CE = −31 eV), and 336.1 → 138.25 (CE = −30 eV). Concentrations (0.001–1 µM) were quantified based on calibration curves prepared using commercially available standards.

2.4. Determination of Kinetic Constants

Kinetic constants were obtained from the SENO concentration-dependent rate for SENO reduction or SEN concentration-dependent rate for SEN clearance as previously described for RIDO[16] and RID.[38,39] The amount of SEN formed was determined as the amount detected in full incubations minus the amount detected in the blanks (without feces or NADPH), while the amount of SEN cleared was determined as the amount detected in blanks (without NADPH) minus the amount in the full incubations. Kinetic constants for SENO reduction by intestinal microbiota and SEN clearance (V_{max} and K_m) were determined by fitting the data to the Michaelis–Menten Equation (1) using GraphPad (GraphPad Prism Software version 5.04, San Diego, CA, USA), where v was rate of reaction (µmol h^{-1} g $feces^{-1}$ or nmol min^{-1} mg^{-1} protein), V_{max} was maximum velocity (µmol h^{-1} g $feces^{-1}$ or nmol min^{-1} mg^{-1} protein), K_m was Michaelis–Menten constant (µM), and S was substrate concentration (µM).

$$v = \frac{v_{max} \times [S]}{K_m + [S]} \quad (1)$$

For SENO reduction by liver S9, the concentration-dependent rate of SENO reduction did not show saturation up to the highest concentration tested. Hence, the data were fitted to Equation (2) with the slope of the linear curve representing the first-order rate constant k which equals V_{max}/K_m when $[S] << K_m$.

$$v = k[S] = \frac{v_{max}}{K_m}[S] \quad (2)$$

2.5. Development of PBK Models

The PBK model for SENO with a SEN submodel was based on the model for RIDO with a submodel for RID[16] (**Figure 2**). Physiological parameters were obtained from literature,[40] and the physicochemical parameters were calculated using available in silico tools such as the Quantitative In Vitro to In Vivo Extrapolation (QIVIVE) tools[41,42] as developed by Wageningen Food Safety Research. Log P values of 0.5 and 1.1 for SENO and SEN, respectively, were taken from PubChem as computed by XLogP3 3.0 (PubChem release 2021.05.07).[43] Due to lack of experimental values, the blood plasma ratio (B/P) is often assumed to be 1 for basic compounds or 0.55 (1-hematocrit) for acidic compounds.[44] Since both SENO and SEN were considered as basic compounds, the B/P ratio was assumed to be 1. The list of parameters and the model code for both the rat and human PBK model can be found in Tables S4, S5, Supporting Information. The model equations were coded and numerically integrated in Berkeley Madonna 9 (UC Berkeley, CA, USA) using Rosenbrock's algorithms for stiff systems to predict AUC_{SEN}.

2.5.1. Absorption

While orally-administered PAs are rapidly absorbed from the GI tract into blood,[18,38,45,46] the more polar PA-N-oxides are more slowly absorbed in the small intestine.[47,48] As a result PA-N-oxides are transferred to a larger extent to the colon, where intestinal microbiota may reduce the PA-N-oxides to the parent PAs prior to absorption via the portal vein to the liver.[16,18,19,46,49–54]

To include all these absorption processes in the PBK models, three types of absorption rate constants were included in the SEN and SENO models: a rate constant for the absorption from the GI tract via the portal vein into the liver (k_{a1} for SENO and k_{b1} for SEN respectively), a rate constant for transfer from the small intestine to the intestinal microbiota compartment located in the colon (k_{in1} for SENO and k_{in2} for SEN respectively), and a rate constant for uptake from the colon compartment to the liver (k_{a2} for SENO and k_{b2} for SEN respectively). As colon was part of the GI tract, k_{a1} was set equal to k_{a2} (labeled $k_{a\,SENO}$) as well as k_{b1} to k_{b2} (labeled $k_{b\,SEN}$). The absorption rate constants for uptake from the GI tract into liver were calculated based on the apparent permeability coefficient (P_{app}) values in Caco-2 cells[48] and an absorption rate constant for uptake of RID from the GI tract to the liver of 0.72 h^{-1}[38] using Equation (3).[16,38,55] The P_{app} values of SENO and SEN were 0.72 (10^{-6} cm s^{-1}) and 16.26 (10^{-6} cm s^{-1}),[48] yielding absorption rate constants for uptake from the GI tract into the liver for SENO ($k_{a\,SENO}$) and SEN ($k_{b\,SEN}$) of 0.17 and 3.90 h^{-1}, respectively. The k_a values thus obtained

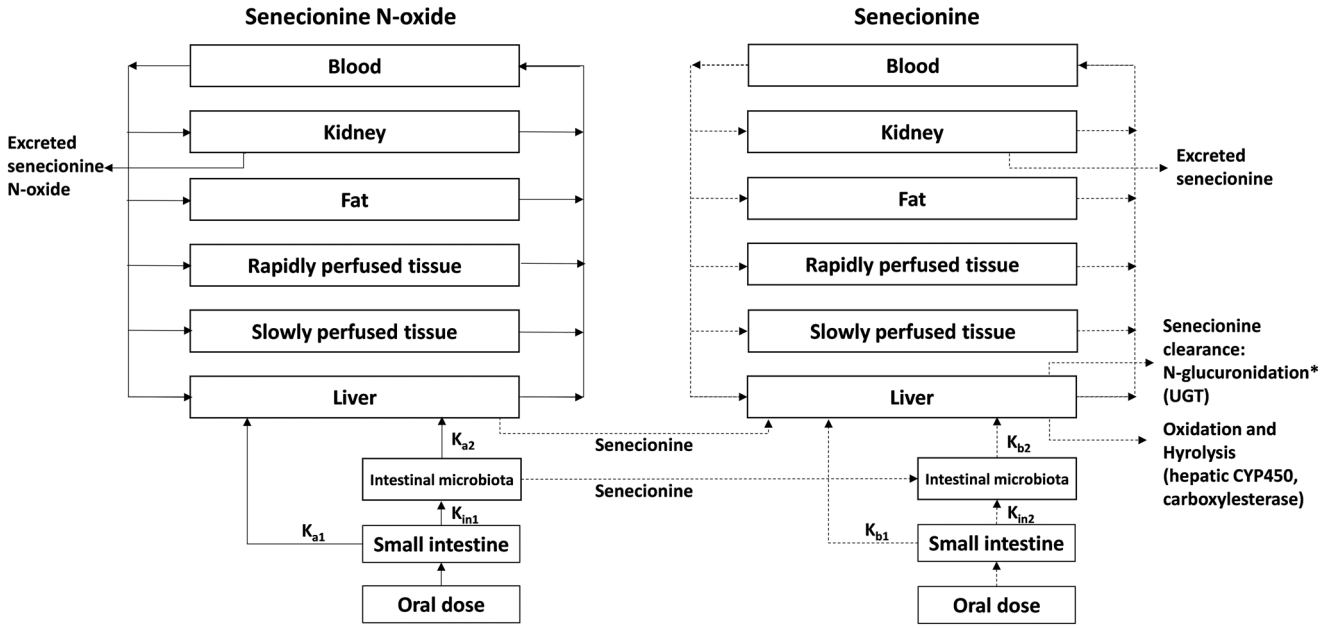

Figure 2. PBK model for SENO with a submodel for SEN. *The N-glucuronidation pathway only occurs in human.

Table 1. Absorption rate values as derived from literature and P_{app} values.

Absorption rate of SENO (k_{a1} and k_{a2})	Absorption rate of SEN (k_{b1} and k_{b2})	Remarks
0.288	0.426	At 11.5 mg SEN kg^{-1} bw[46]
0.276	0.330	At 5.7 mg SEN kg^{-1} bw[46]
0.170	3.900	P_{app}[48] and k_a values based on Equation (3).[16,38,55]
0.245	1.552	Average value from literature as final k_a or k_b values

were compared to and combined with other reported absorption rate values from Wang et al.,[46] and an average value was taken for the PBK model as shown in **Table 1**. The transfer rate constants of SENO and SEN from the small intestine (lower ileum) to the intestinal microbiota (caecum) (k_{in1} for SENO and k_{in2} for SEN) were assumed to be the same as the rate constants for transfer of orally-administered drugs, amounting to 0.46 h^{-1}.[16,37,56]

$$\frac{P_{\text{app PA or PA N-oxides}}}{k_{a\ \text{PA or PA N-oxides}}} = \frac{P_{\text{app RID}}}{k_{a\ \text{RID}}} \quad (3)$$

2.5.2. Metabolism

Kinetic constants for four metabolic conversions were included in the PBK models namely for SENO reduction to SEN 1) by intestinal microbiota and 2) in the liver, and for SEN clearance in the liver through 3) oxidation and hydrolysis by hepatic CYP450 and carboxylesterase (i.e., liver S9), and 4) through N-glucuronidation by UGT (Figure 2). N-glucuronidation was only considered in the human PBK model as it was reported to not occur in rats.[22,35] The SENO reduction to SEN by intestinal CYP450 was not included in the PBK model because the rate of this reaction was significantly lower than liver CYP450 reduction.[16,17] When converted to in vivo or the whole body, SENO reduction by intestinal CYP450 amounted to only 8.3% of that by liver tissue.

Scaling of the in vitro V_{max} and catalytic efficiency (k_{cat} or V_{max}/K_m) to the in vivo situation was performed for both incubations with feces and S9. For SENO reduction by intestinal microbiota, the in vitro V_{max} (μmol h^{-1} g^{-1} feces) was scaled to the whole body using Equation (4) and a fecal fraction to body weight (fbw) of 0.0164 g rat feces g^{-1} bw based on a defecation volume per day of 4.1 g and a bw of 250 g,[37,57,58] or of 0.0018 g human feces g^{-1} bw based on a defecation volume per day of 128 g and a default bw of 70 kg.[58,59] Fecal microbiota was used as first approach to represent intestinal microbiota because feces was previously shown to best mimic the cecal content where the majority of microorganisms resides,[16,37,58,60] and also because use of fecal incubations combined with scaling based on defecation rates as the methodology for converting the in vitro data obtained to the whole body has been proven adequate in previous studies.[16,37,58,60,61]

$$V_{max}\text{in vivo} = V_{max}\text{in vitro} \times \text{fbw} \times 1000 \quad (4)$$

For SENO reduction and SEN clearance by liver S9, in vitro V_{max} and k_{cat} values were scaled based on Equation (5) using an S9 protein yield of 143 mg S9 protein g^{-1} liver for rat[62] (based on the sum of 108 mg microsomal protein g^{-1} tissue and 35 mg cytosolic protein g^{-1} tissue), or 120.7 mg S9 protein g^{-1} liver for human[63] (based on the sum of 40 mg microsomal protein g^{-1} tissue and 80.7 mg cytosolic protein g^{-1} tissue). For SENO reduction by small intestine S9, the in vitro k_{cat} was scaled using an S9 protein yield of 38.6 mg S9 g^{-1} intestine tissue[63] (based on the sum of 20.6 mg microsomal protein g^{-1} tissue and 18 mg cytosolic protein g^{-1} tissue). The K_m values in vivo were assumed to be

similar to those obtained in vitro. For SEN clearance by UGTs, kinetic parameters were obtained from literature and were scaled with Equation (5) using a human liver microsomal yield of 40 mg microsomal protein g^{-1} tissue.[22,35]

$$k_{cat}\text{ in vitro} = \frac{V_{max}\text{ in vitro}}{K_m},$$

$$k_{cat}\text{ in vivo} = \frac{k_{cat}\text{ in vitro} \times 60 \times \left[\text{fraction of } S9 \text{ or microsome in organ}\right] \times \left[\text{organ weight}\right]}{1000} \quad (5)$$

2.5.3. Excretion

In the PBK models, urinary excretion was described by glomerular filtration (GF)[16,64,65] as in Equation (6) using a glomerular filtration rate (GFR) of 0.08 L h^{-1} in rat and 7.5 L h^{-1} in human,[64] and the fraction unbound (F_{ub}) values of SENO and SEN of 0.987 and 0.491, respectively.[41,66] F_{ub} values were quantified using an in silico QIVIVE tool,[41] and the values for rat and human were assumed to be similar.

$$GF_{PA\text{ or }PA\ N-oxides} = GFR \times \left(CVK_{PA\text{ or }PA\ N-oxides} \times Fub_{PA\text{ or }PA\ N-oxides}\right) \quad (6)$$

2.5.4. Dose and Bioavailability for Evaluation of Model Predictions

For model validation by comparison to available literature data on kinetics, an equimolar dose of 55 μmol kg^{-1} bw SENO or SEN was used, based on the dose used in the in vivo study reported by Yang et al.[11] The SEN submodel was validated using three dose levels of 22.9, 11.5, and 5.7 mg kg^{-1} bw representing the dose levels used in the in vivo study reported by Wang et al.[46] Simulations were performed assuming the 8.2% bioavailability upon oral dosing previously reported for SEN,[46] unless indicated otherwise. For evaluation of the predicted REP value PBK model calculations were performed at a dose of 55 μmol kg^{-1} bw since this was the dose level used in the in vivo experiments for which kinetic data were available. The REP value was calculated as the ratio between the area under the SEN blood concentration time curve (AUC_{SEN}) predicted by the PBK model for rats orally-administered with SENO and the AUC_{SEN} predicted upon dosing an equimolar dose of SEN as depicted in Equation (7). Given that the REP value was dose-dependent as shown in the previous study,[16] the study used a range of doses including low realistic exposure levels starting from 0.1 mg kg^{-1} bw to[21,67] high doses as used in animal studies up to 300 mg kg^{-1} bw[68,69] to investigate the dose-dependent REP value of SENO to SEN in rat and human.

$$REP_{SENO\text{ in rat or human}} = \frac{AUC_{SEN}\text{from orally dosed senecionine N} - \text{oxide}}{AUC_{SEN}\text{from orally dosed senecionine}} \quad (7)$$

2.6. Sensitivity Analysis

A sensitivity analysis was performed to assess which parameters of the PBK model have the largest impact on the predicted AUC_{SEN} at 24 h. Normalized sensitivity coefficients (SCs) were calculated[70] using Equation (8) where C was the initial value of the model output, C' was the modified value of model output with a 5% increase of an input parameter, P was the initial parameter value and P' was the parameter value with an increase of 5%. Only one parameter was changed each time, while the other parameters were kept at their initial values. A large SC value indicates that the respective parameter has a large impact on the predicted AUC_{SEN}. An equimolar dose of 55 μmol kg^{-1} bw (either 19.33 mg kg^{-1} bw SENO or 18.45 mg kg^{-1} bw SEN) used in the animal study of Yang et al.,[11] or 0.285 μmol kg^{-1} bw (either 0.1 mg kg^{-1} bw SENO or 0.095 mg kg^{-1} bw SEN) representing the lower bound of PA exposure levels with human relevance,[21,67] was used to perform the sensitivity analysis in the rat and human model, respectively. All sensitivity analyses were performed assuming a bioavailability of 8.2%.

$$SC = \frac{(C' - C)}{(P' - P)} \times \frac{P}{C} \quad (8)$$

3. Results

3.1. In Vitro Kinetic Data for Rat and Human

The in vitro kinetic data for SENO reduction to SEN in incubations with rat and human fecal samples (**Figure 3**a) and liver S9 (Figure 3b), and the in vitro V_{max}, K_m, and k_{cat} values derived from these curves along with the scaled values are summarized in **Tables 2** and **3**. The results obtained in Figure 3a show that the concentration-dependent rate of SENO reduction to SEN by fecal samples followed Michaelis–Menten kinetics. Although the in vitro k_{cat} for reduction of SENO by intestinal microbiota from human is 7.2-fold higher compared to the in vitro k_{cat} for reduction of SENO by intestinal microbiota from rat, the scaled in vivo k_{cat} is 1.3-fold lower in human than rat due to the relatively lower 24-h defecation volumes in human.

Figure 3b reveals that the concentration-dependent rate of SENO reduction by rat and human liver S9 followed first-order reaction kinetics, while data obtained for the concentration dependent SENO reduction by rat small intestine S9 can be found in Figure S7, Supporting Information. Although the in vitro k_{cat}

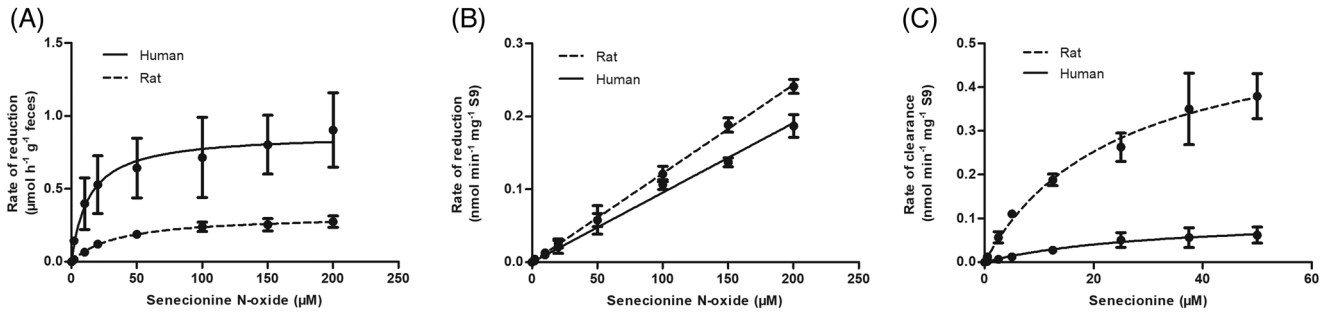

Figure 3. SENO concentration-dependent rate of SEN formation in a) anaerobic incubation with pooled feces or b) aerobic incubation with liver S9. SEN concentration-dependent rate of c) SEN clearance in aerobic incubation with liver S9. Data are presented as mean ± SD of three independent experiments ($n = 3$) with feces or liver S9 of rat and human.

Table 2. Kinetic constants for SENO reduction by intestinal microbiota in rat and human.

	Rat	Human
V_{max}, in vitro [μmol h^{-1} g^{-1} feces]	0.320 ± 0.005	0.877 ± 0.038
V_{max}, in vivo [μmol h^{-1} kg^{-1} bw][a)]	5.250 ± 0.088	1.578 ± 0.068
K_m [μM]	35.090 ± 1.960	13.360 ± 2.630
k_{cat}, in vitro [L h^{-1} g^{-1} feces][b)]	0.009	0.066
k_{cat}, in vivo [L h^{-1} kg^{-1} bw][c)]	0.150	0.118

[a)] V_{max} in vivo = (V_{max}, in vitro) × fbw × 1000. Fraction of feces to bw for rat and human are 0.0164[37,57,58] and 0.0018[58,59] g feces g^{-1} bw, respectively; [b)] k_{cat}, in vitro = (V_{max}, in vitro)/K_m; [c)] k_{cat}, in vivo = ($V_{max,}$ in vivo)/K_m.

values for reduction of SENO by liver S9 are relatively similar in both species, the scaled in vivo k_{cat} is 1.9-fold lower in human than in rat due to relatively lower level of S9 in human liver than in rat liver. In rat, the in vivo k_{cat} values of SENO reduction by liver S9 were 2.3-fold and 12.0-fold higher than the in vivo k_{cat} values for SENO reduction by the intestinal microbiota and by small intestine S9, respectively. In human, the scaled in vivo k_{cat} value for SENO reduction by liver S9 was 1.6-fold higher than the k_{cat} for reduction by the intestinal microbiota. Based on the trend found in rat and a previous study by Ning et al.[39] showing the PA metabolism in small intestine to be significantly lower than that in the liver, SENO reduction by the small intestine was not included in the PBK models.

The in vitro kinetics for SEN clearance in incubations with rat and human liver S9 are presented in Figure 3c and Table 3 along with the scaled in vivo V_{max} and k_{cat} values.

Figure 3c shows that the concentration-dependent rate of SEN clearance followed Michaelis–Menten kinetics. The in vitro k_{cat} value for clearance of SEN by liver S9 is 6.7-fold lower for human than rat liver S9. Similarly, the in vivo k_{cat} value is 11.2-fold lower in human than in rat. These overall lower clearance k_{cat} values in human were mainly due to a relatively lower V_{max} and lower S9 protein for human liver than for rat liver. In the next step, all obtained kinetic parameters were integrated in the PBK models to examine if these kinetic differences result in different REP values of SENO relative to SEN for rat and human.

3.2. PBK Model Validation

To validate the PBK model, the model outcome is compared with the animal data as reported by Yang et al.[11] and Wang et al.[46] as shown in **Table 4**. **Figure 4** compares the PBK model simulation with published in vivo animal data from Yang et al.[11] assuming 8.2% bioavailability, as reported upon oral exposure of rat to SENO or SEN. Using an equimolar oral dose of 55 μmol kg^{-1} bw of either SENO or SEN, blood concentrations of SENO and SEN, or of only SEN, were simulated. Figure 4a reveals that the model predictions underestimated the maximum SENO blood concentration ($C_{max\ SENO}$) reported by Yang et al.[11] by a factor

Table 3. Kinetic constants for S9 or microsomal metabolism in rat and human.

	Rat			Human		
	SENO reduction		SEN clearance	SENO reduction	SEN clearance	
	Liver S9	Small intestine S9	Liver S9	Liver S9	Liver S9 (CYP450 and carboxylesterases)	Liver microsome (N-glucuronidation)[d)]
V_{max}, in vitro [nmol min^{-1} mg^{-1} protein]	n.a.	n.a.	0.560 ± 0.040	n.a.	0.100 ± 0.010	3.000 ± 0.150
V_{max}, in vivo [μmol h^{-1} kg^{-1} bw][a)]	n.a.	n.a.	163.360 ± 11.670	n.a.	18.830 ± 1.880	187.200 ± 9.360
K_m [μM]	n.a.	n.a.	24.390 ± 3.650	n.a.	31.370 ± 6.150	710.000 ± 70.000
k_{cat}, in vitro [mL min^{-1} mg^{-1} protein][b)]	0.001	0.001	0.020	0.001	0.003	0.004
k_{cat}, in vivo [L h^{-1} kg^{-1} bw][c)]	0.350	0.029	6.700	0.188	0.600	0.264

[a)] $V_{max,}$ in vivo = [(V_{max}, in vitro)/1000] × 60 × [S9 or microsome in organ] × [organ weight]. Rat S9 is 143 mg S9 g^{-1} liver and 38.6 mg S9 g^{-1} small intestine. Human hepatic fraction is 120.7 mg S9 g^{-1} liver and 40 microsome g^{-1} liver. The weight of rat liver, small intestine, and human liver are 34, 14, and 26 g kg^{-1} bw, respectively; [b)] k_{cat}, in vitro = (V_{max}, in vitro)/K_m; [c)] k_{cat}, in vivo = (V_{max}, in vivo)/K_m; [d)] He et al.[35]

Table 4. PBK model outcome compared to animal data as reported by Yang et al.[11] and Wang et al.[46] assuming 8.2% bioavailability and a rat bw of 0.20 kg[13] or of 0.25 kg.[46].

Parameters	Oral dose of SENO		Oral dose of SEN							
Oral dose [mg kg^{-1} bw]	19.33		18.45		22.9		11.5		5.7	
	PBK model	Animal data (Yang et al.)[11]	PBK model	Animal data (Yang et al.)[11]	PBK model	Animal data (Wang et al.)[46]	PBK model	Animal data (Wang et al.)[46]	PBK model	Animal data (Wang et al.)[46]
$C_{max\ SENO}$ [ng mL^{-1}]	232.98	392.29	n.a.	n.a.	n.a.	n.a.	n.a.	n.a.	n.a.	n.a.
$T_{max\ SENO}$ [h]	1.05	3.56	n.a.	n.a.	n.a.	n.a.	n.a.	n.a.	n.a.	n.a.
$C_{max\ SEN}$ [ng mL^{-1}]	56.31	38.66	191.47	205.79	231.46	1226.69	114.58	451.37	56.38	412.11
$T_{max\ SEN}$ [h]	1.05	0.67	0.26	0.17	0.26	0.17	0.26	0.17	0.26	0.17
AUC_{SEN} [ng mL^{-1} h]	176.01	251.80	217.69	287.33	272.85	1278.67	135.54	552.33	66.81	502.17
REP (as ratio of AUC_{SEN})	n.a.	n.a.	0.81[a]	0.88	n.a.	n.a.	n.a.	n.a.	n.a.	n.a.
$AUC_{pyrrole\text{-}protein}$ [ng mL^{-1} h]	n.a.	6416.33	n.a.	10474.67	n.a.	n.a.	n.a.	n.a.	n.a.	n.a.
REP (as ratio of $AUC_{pyrrole\text{-}protein}$)	n.a.	n.a.	n.a.	0.61	n.a.	n.a.	n.a.	n.a.	n.a.	n.a.

n.a., not applicable. [a] REP value is 0.81 or 0.83 when calculated with either 0.2 kg or 0.25 kg as bodyweight, respectively.

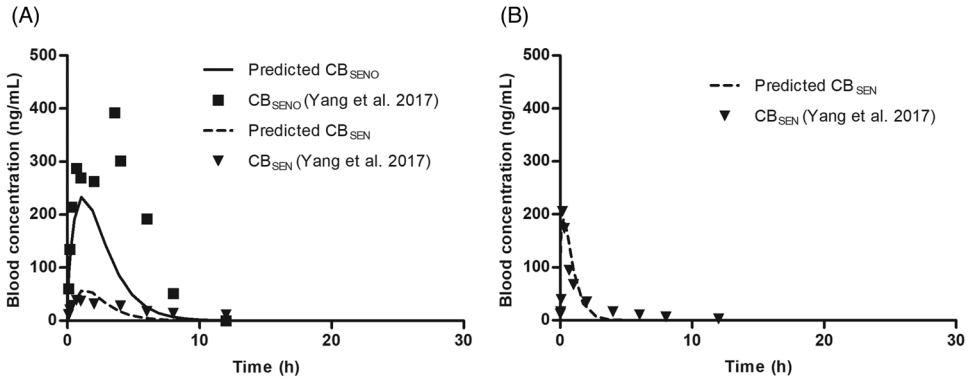

Figure 4. PBK model predicted and literature reported data for the C_{max} of SENO and SEN upon an equimolar oral dose of a) 19.33 mg kg^{-1} bw SENO or b) 18.45 mg kg^{-1} bw SEN as used in the in vivo study by Yang et al.[11] with a bioavailability of 8.2% and rat body weight of 0.20 kg.

of only 1.7-fold while the maximum SEN blood concentration ($C_{max\ SEN}$) upon oral SENO administration was slightly overestimated by a factor of 1.4-fold compared to the $C_{max\ SEN}$ reported by Yang et al.[11] Figure 4b reveals that when SEN was orally-administered, the model outcomes closely matched the $C_{max\ SEN}$ reported by Yang et al.[11] Assuming 100% bioavailability appeared to overpredict the literature data (Figure S8, Supporting Information).

To validate the model further, **Figure 5** compares the PBK SEN submodel predictions with published in vivo animal data from Wang et al.,[46] again assuming 8.2% bioavailability. The simulated outcome with 100% bioavailability can be found in Figure S9, Supporting Information. In this model validation, three different doses of SEN were used to mimic the conditions used in the animal studies. In contrast to the well-fitted outcome shown in Figure 4b, the PBK model predictions of $C_{max\ SEN}$ underestimated the C_{max} reported in the study from Wang et al.[46] by 3.9–7.3-fold for the three doses.

3.3. PBK Model Prediction

The PBK model based predictions of SEN toxicokinetic profile in rat and human with 8.2% bioavailability are shown in **Figure 6**a,b, respectively. The profile with 100% bioavailability can be found in Figure S10, Supporting Information. Figure 6a and Table 4 reveal that the rat PBK model predicted lower $C_{max\ SEN}$ and a more delayed $T_{max\ SEN}$ upon orally-administered SENO compared to the situation upon orally-administered SEN. A similar trend is also found for the human PBK model predictions as shown in Figure 6b. Comparison of the predicted rat and human data reveals a notable difference with significantly higher $C_{max\ SEN}$ values and prolonged exposure to SEN in human as compared to rat.

Figure 7a,b shows the dose-dependent REP values of SENO in rat and in human calculated based on the ratio of AUC values derived from the predicted time-dependent SEN concentration–time profiles presented in Figure 6a,b. The REP values derived from an available in vivo study that reports AUC_{SEN} values

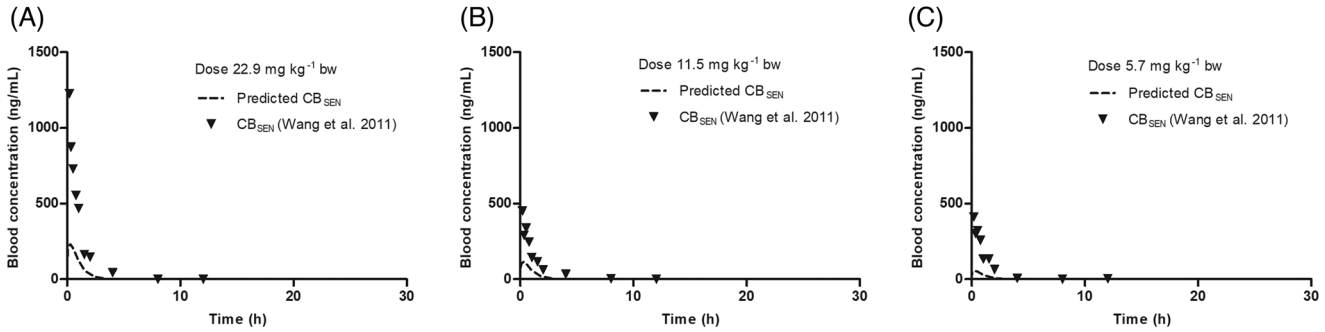

Figure 5. PBK model predicted and literature reported data for the $C_{max\ SEN}$ upon oral doses of a) 22.9, b) 11.5, and c) 5.7 mg kg^{-1} bw SEN as used in the in vivo study by Wang et al.[46] with a bioavailability of 8.2% and rat body weight of 0.25 kg.

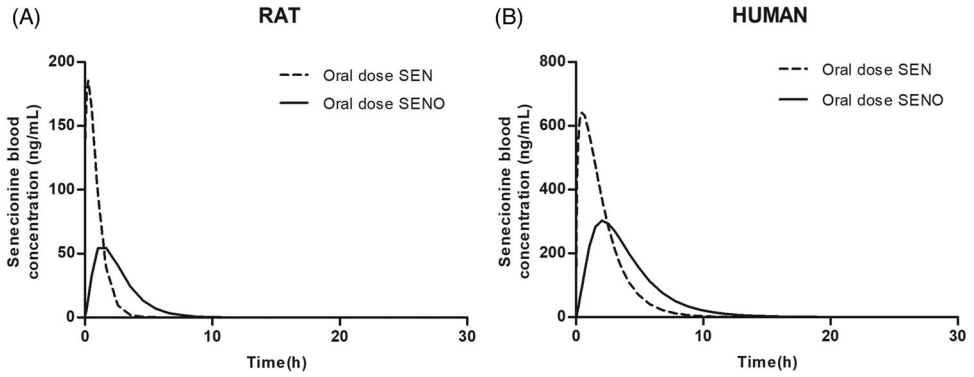

Figure 6. PBK model predicted concentration–time toxicokinetic profile of SEN in blood of a) rat and b) human with 8.2% bioavailability at equimolar dose of 19.33 mg kg^{-1} bw SENO (continuous line) or 18.45 mg kg^{-1} bw SEN (dashed line). Note the unequal scaling of the two y-axis.

and $AUC_{pyrrole\text{-}protein}$ levels upon dosing either SEN or SENO[11] (Table 4) are also depicted. From the results thus obtained it follows that: 1) these REP values derived from the in vivo data closely match the PBK-model based predicted REP values, and 2) the in vivo REP value calculated based on the ratio of the literature reported $AUC_{pyrrole\text{-}protein}$ values (0.61) is lower than the REP value calculated based on the ratio of the literature reported AUC_{SEN} values (0.88). The results also reveal that at realistic low dose exposure scenarios, the REP value of SENO predicted based on the ratio of the AUC_{SEN} amounted to be 0.84 in rat, and to 0.89 in human. Meanwhile at high dose level of 55 μmol kg^{-1} bw used in animal study,[11] the interspecies difference appeared somewhat smaller with REP values amounting to 0.83 for rat and 0.86 for human, respectively. The results in Figure 7 also reveal that regardless of the bioavailability value used, at realistic low dose levels the REP values converge to a comparable value for both species.

To investigate the reason behind the dose-dependent decrease of the REP value with increasing dose levels, in **Figure 8**, the normalized AUC_{SEN} (calculated as the AUC_{SEN} divided by the dose) is

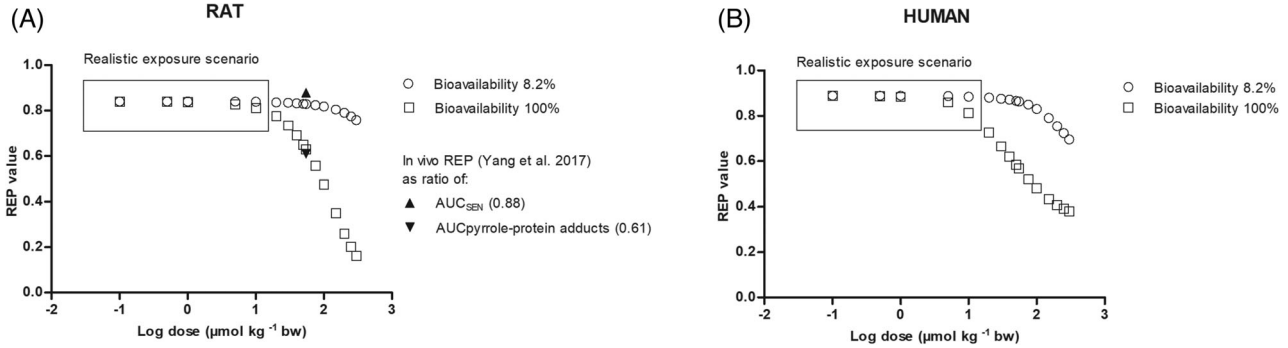

Figure 7. REP values calculated as the ratio of the PBK model predicted AUC_{SEN} upon an oral dose of SENO and the AUC_{SEN} upon an equimolar oral dose of SEN, where the REP value is plotted against the log equimolar dose (μmol kg^{-1} bw) of SENO and SEN in a) rat and b) human assuming different bioavailability of 8.2% and 100%. For comparison the REP values derived from the in vivo experimental rat data from Yang et al.[11] (Table 4) are also presented.

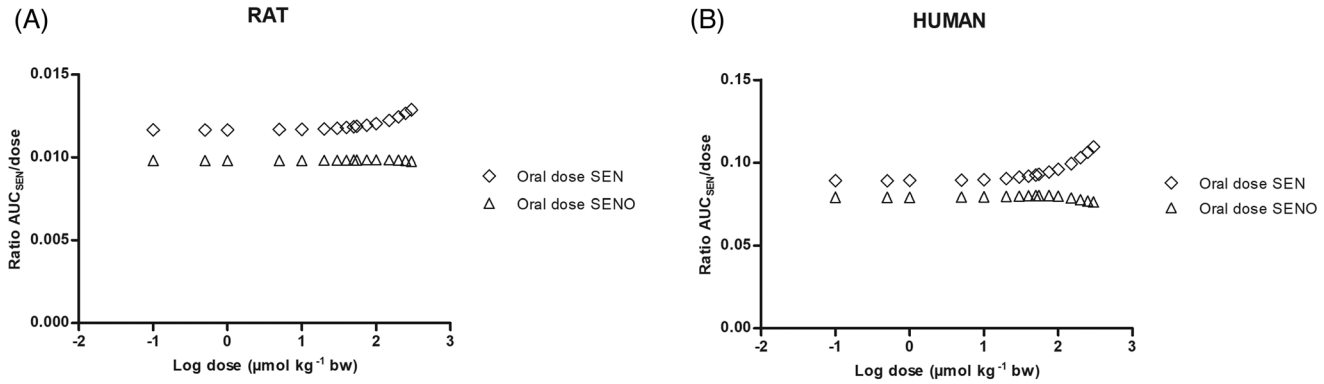

Figure 8. Ratio of AUC_{SEN}/dose against log equimolar dose (μmol kg^{-1} bw) in a) rat and b) human with 8.2% bioavailability after oral dose of SENO and of SEN. Note the unequal scaling of the two *y*-axis.

plotted against the oral dose of SENO or of SEN. From these data it follows that in both species, with increasing dose of SEN, the AUC_{SEN} increases more than proportional with the dose pointing at saturation of SEN clearance. This saturation effect is less pronounced when dosing SENO: with increasing dose of SENO, the reduction of SENO to SEN may saturate resulting in a decline of the AUC_{SEN} with increasing dose of SENO. Together the saturation of SEN clearance and of SENO reduction result in decreasing REP values at higher doses in both species.

3.4. Sensitivity Analysis

To evaluate the model's sensitivity, normalized SCs were calculated for both the SENO and SEN model at high dose in rat and low dose in human resulting in the data shown in **Figure 9**. Independent of the dose and species, similar results are obtained. In the SENO model, the parameters of high influence on the model predictions for the AUC_{SEN} at 24 h are those involved in the reduction of SENO and the clearance of SEN by liver S9. Similar to the rat model, and given that SEN is also cleared through N-glucuronidation in human, these clearance-related parameters were also demonstrated to be influential in the human model. In the SEN model, the influential parameters are mainly related to SEN clearance by liver S9 and by N-glucuronidation. It is worth noting that in the human model the SEN clearance by liver S9 is relatively more influential than SEN clearance by N-glucuronidation.

4. Discussion

The aim of this study was to investigate whether previously published NAM to quantify REP values for a PA-N-oxide relative to its parent PA using PBK models[16] can also be applied to i) calculate the REP value of another PA-N-oxide than RIDO, using SENO and SEN as the model compounds, and ii) to investigate if interspecies differences in metabolic capacity between rat and human also result in different REP values. Compared to the REP value at low dose exposure levels previously defined for rats using a similar in vitro-in silico NAM for RIDO as compared to RID of 0.78,[16] the REP value now obtained for SENO relative to its parent PA SEN of 0.84 is slightly higher. Yet, similar to RIDO, the predicted REP value of SENO is lower than 1, amounting at realistic low dose levels to 0.84 in rat and 0.89 in human. Despite the interspecies differences in metabolic kinetic parameters, the REP values at realistic low dose exposure appeared comparable in both species.

Compared to the previous results obtained for RIDO, the kinetic parameters obtained in the present study for the reduction of SENO by rat samples show that in anaerobic rat fecal incubations the reduction of SENO occurs 6.7-fold slower than that of RIDO, whereas in incubations with liver S9 it is 2.4-fold faster. It is worth highlighting that the in vivo k_{cat} value for SENO reduction by intestinal microbiota is lower than by liver, in contrast to what was observed for reduction of RIDO for which the reduction by intestinal microbiota appeared to exceed that by the liver. Consistent with previous studies, N-oxide reduction by small intestine S9 appeared substantially less efficient than that by liver S9[16,17] an observation that can be related to the fact that reduction of PA-N-oxides is reported to be mainly facilitated by CYP1A2 and CYP2D6,[17] which show lower activity in rat intestinal microsomes than rat liver microsomes.[71] A similar trend was also observed for human samples, for which N-oxide reduction by small intestine S9 was relatively small and therefore not included in the PBK model.[39] When converted to in vivo k_{cat} values with appropriate scaling factors for either microsome or S9, the clearance of SEN in rat liver (6.70 L h^{-1} kg^{-1} bw) appears to be faster than that of RID (2.0 L h^{-1} kg^{-1} bw). The finding is in agreement with previous literature where Geburek et al. (2020) associated an extra -OH group with higher degree of oxidation and consequently lower degradation as seen in RID compared to SEN.[72]

It is of interest to note that also PAs were reported to be metabolized by the intestinal microbiota. For instance, literature reports that PAs can be converted by intestinal microbiota to a 1-methylene derivative, namely 7*α*-hydroxy-1-methylene-8*α*-pyrrolizidine[47,73,74] or oxidized to its N-oxide.[46] Yet, these metabolic conversions were not included in the model because formed PAs were shown to be stable upon incubation with intestinal microbiota showing negligible clearance in incubations with both rat and human feces as shown in Figures S1, S2, Supporting Information, respectively. Rather, PAs in the

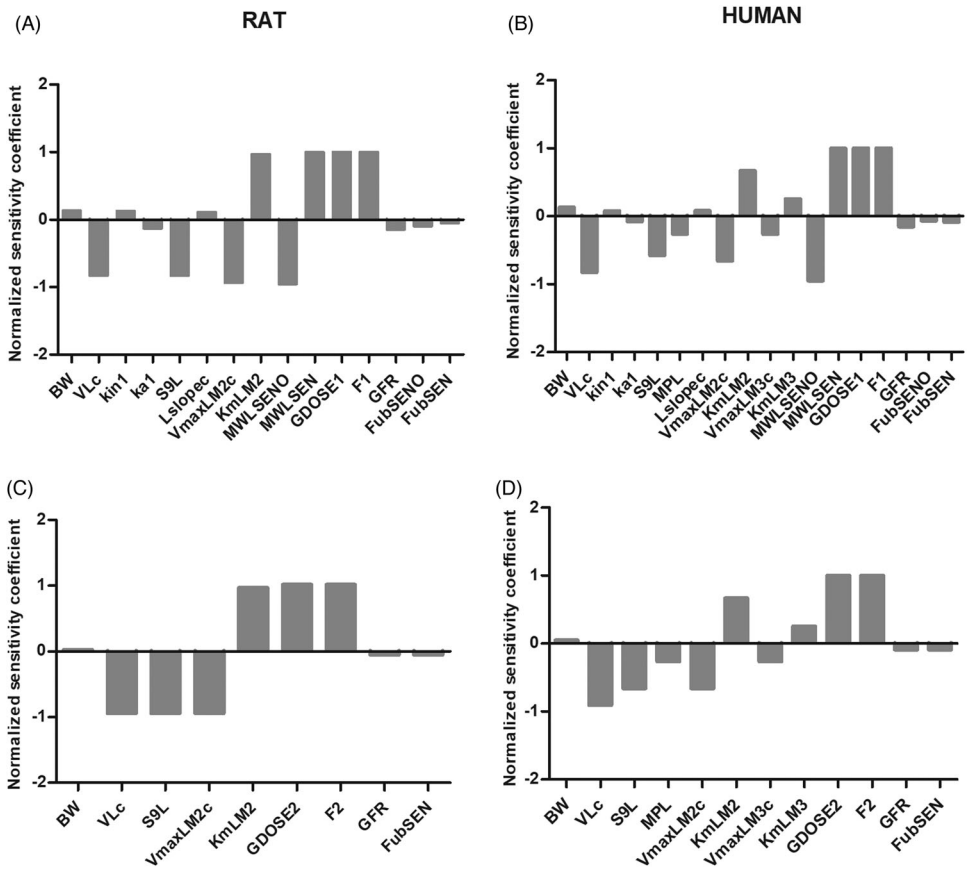

Figure 9. Normalized SCs for the parameters of the a–c) rat and b–d) human PBK model for SENO (top) and SEN (bottom) on predicted AUC_{SEN} at 24 h (ng mL^{-1}) in blood at equimolar doses of either 55 μmol kg^{-1} bw in rat or 0.285 μmol kg^{-1} bw in human with assumed 8.2% bioavailability. The complete list of abbreviations can be found in Tables S4, S5, Supporting Information.

intestinal tract are quickly absorbed into the liver via the portal vein.[11,16,19–21,75]

When kinetic parameters for SENO reduction obtained in anaerobic liver S9 incubations (Table S2 and Figure S3, Supporting Information) were used as model input, the model predicted a $C_{max\,SENO}$ that was 4.4-fold lower and a $C_{max\,SEN}$ that was 1.9-fold higher than the C_{max} from the animal data, compared to a 1.7-fold and 1.4-fold difference obtained with the aerobic rate constants (Figure S4, Supporting Information). Moreover, the predicted REP value at 8.2% bioavailability with aerobic kinetic results (0.83) (Figure S5, Supporting Information) is closer to the animal-study result (0.88), than the REP value obtained with the anaerobically obtained kinetic constants (0.96) (Table S2, Supporting Information). Thus, it is concluded that the aerobic conditions apparently better reflect the partly aerobic conditions in liver tissue. A similar result was previously obtained for RIDO.[16]

Similar to the experiments performed under anaerobic condition, changing the current methodology by using NADPH regeneration system instead of NADPH did not improve the model-predicted kinetic profile and REP values compared to reported animal data as shown in Table S3, Supporting Information. Instead, the model-predicted toxicokinetic profile for both SENO and its PA upon oral SENO dosage showed a worse fit to the animal data (Figure S6a, Supporting Information), with the model-predicted $C_{max\,SENO}$ being 4.2-fold lower and the $C_{max\,SEN}$ 1.9-fold higher than the reported animal data (compared to a 1.7-fold and 1.4-fold difference with NADPH) (Figure S6b, Supporting Information). Moreover, the predicted REP value at the reported 8.2% bioavailability obtained with the NADPH dependent kinetic parameters (0.83) was closer to the animal-study result (0.88), than the REP value predicted using the kinetic constants obtained with the NADPH regeneration system providing a REP value of (0.96) (Table S3, Supporting Information). Given that the PBK model is a model and should predict the in vivo data as good as possible, it was concluded that the data obtained with NADPH under aerobic conditions provide the best possible predictions for the in vivo situation. Nevertheless, the finding that also for PA-N-oxides an NADPH regeneration system results in a higher catalytic efficiency for reduction in microsomal incubations is worth further investigations to also elucidate the underlying mode of action and enzymes involved, which may be similar to the mode of action and reductases reported by Mazur et al. for carbonyl compounds.[76]

Upon validating the SEN submodel for rat, the PBK model based prediction better matched the reported animal data from Yang et al.[11] while the simulated outcomes underestimate the

reported data from Wang et al.[46] Despite the comparable dose levels of 18.45 mg kg^{-1} bw SEN and 22.9 mg kg^{-1} bw SEN in the studies of Yang et al.[11] and Wang et al.,[46] respectively, the C_{max} in the latter study was 6.0-fold higher. This larger deviation may in part be ascribed to variability in the experimental data such as inclusion of fasting[46] or injection of saline solution as a replacement of a taken blood sample.[11] Alternatively, since the values as reported by Wang et al.[46] seemed to be relatively high, bioavailability in the Wang et al.[46] study may have been even higher than 8.2%.

Compared with the human model, the kinetic parameters used as input for the rat model generally show faster metabolism in N-oxide reduction and PA clearance. Although the in vitro catalytic efficiency of SENO reduction by intestinal microbiota in human is higher than that in rat, the in vivo catalytic efficiency shows the opposite trend due to a higher fraction of feces to bodyweight in rat. This higher in vitro catalytic efficiency for intestinal microbial N-oxide reduction in human than in rat concords with an in vitro study performed on the drug loperamide N-oxide, which showed faster N-oxide reduction in human ileal effluents than in rat gut content.[77] Despite interspecies differences in fecal residence time, where feces resides for 8[78] and 30–40 h[79] in rat and human, respectively, our PBK models predicted the transformation time of SENO to SEN to be complete upon 7.9 h in rat and upon 12.6 h in human. This leads to the conclusion that SENO is expected to be fully converted to its parent PA within the fecal residence time for both species. The main bacterial species responsible for PA-N-oxide reduction by the intestinal microbiota remain to be elucidated, but a study with another N-oxide (trimethylamine N-oxide) reported Enterobacteriaceae, particularly *Escherichia coli*, to be the main cause for N-oxide reduction. Yet, the amount of fecal Enterobacteriaceae in human and rat are similar,[80] amounting to approximately 6 $\log_{10}$ cfu per gram feces, and can thus not explain the interspecies difference in catalytic efficiency observed in our in vitro results. Consequently, the role of other bacteria genera or enzymes such as fecalases, cecalases, and gut microbiota reductases in PA-N-oxide reduction should be further investigated. PA-N-oxide reduction also takes place in the liver, with the catalytic efficiency in in vitro incubations with liver S9 being higher in rat than in human. This finding agrees with a previous study where rat liver microsomes reduced the drug benfluron N-oxide to benfluron 5-fold faster than human liver microsomes.[81] The enzymatic activity of CYP1A2 and CYP2D6, which catalyze N-oxide reduction, are also higher in rat liver microsomes than in human liver microsomes,[71] which further explains this interspecies difference. Additionally, the clearance of the formed parent PA SEN appeared to be faster in incubations with rat liver S9 than with human liver S9. This finding corroborates the observation reported by Kolrep et al.[82] that SEN is cleared faster and to a higher extent by rat liver S9 than by human liver S9, and is also in line with what was reported for other PAs by Ning et al.[39] Furthermore, SEN is metabolized by CYP3A4,[83] a predominant isoenzyme present in the liver, and CYP3A4 contributes to the majority of CYP3A activity.[84] The enzymatic activity of CYP3A was reported to be higher in rat liver microsomes than in human liver microsomes,[71] explaining the faster clearance of SEN in rat than human. The PBK model predicted a different kinetic profile for SEN in human as compared to rat with a significantly higher $C_{max\ SEN}$ and prolonged exposure, which are in line with results reported before from human PBK model built for senkirkine,[85] lasiocarpine and riddelliine.[39]

In spite of these substantial interspecies differences in metabolic clearance and kinetics of SENO and SEN, the differences in the predicted REP values appeared limited. The time-dependent profiles for the $C_{max\ SEN}$ upon dosing equimolar amounts of SENO or SEN are similar in rat and human: a lower $C_{max\ SEN}$ and a delayed $T_{max\ SEN}$ in case of dosing SENO as compared to the kinetic profile obtained upon dosing SEN. In contrast to previous studies where an in vivo REP value was derived from the ratio of DHP-DNA adducts formed upon dosing equimolar doses of the N-oxide and parent PA,[16,19,20,28] the current study used both the ratio of the AUC_{SEN} (0.88) or the ratio of $AUC_{pyrrole\text{-}protein}$ (0.61) in rats orally-administered with SENO to those orally-administered SEN to calculate the in vivo REP values because pyrrole-protein (DHP-protein) adducts can also be used as biomarkers of toxic PA exposure.[15,86,87] In addition, Xia et al.[87] showed that the level of DHP-DNA adducts correlated with the level of pyrrole-protein adducts, with correlation coefficients of 0.573–0.702 and p values of 0.07–0.02.

In theory, using the $AUC_{pyrrole\text{-}protein}$ would be a better approach than using the AUC_{SEN} to calculate the REP value because adducts may reflect the toxicity of PA exposure better than the parent PAs themselves. Yet, at the present state of the art this approach is hampered by the fact that the $AUC_{pyrrole\text{-}protein}$ can so far be determined only using in vivo animal studies. To develop a PBK modeling based approach to derive and predict the $AUC_{pyrrole\text{-}protein}$ and the related REP value is a new study in itself that is of interest for future research. Moreover, it is of interest to note that when using the ratio of $AUC_{pyrrole\text{-}protein}$ quantified in an experimental rat study[11] to calculate the REP value, a value of 0.61 is obtained, which is lower than the value of 0.88 obtained when using the AUC_{PA} from the same rat study (Table 4). This discrepancy may be due to depletion of internal GSH at high dose level of PAs,[88–91] thereby exceeding the capacity of pyrrole-GSH conjugation and instead forming more pyrrole-DNA or pyrrole-protein adducts. It may in theory also be due to saturation of the glutathione conjugation by glutathione S-transferases at high internal PA concentrations. Given that $C_{max\ SEN}$ was shown to be higher when dosing SEN as compared to dosing an equimolar dose of SENO (Figure 6), this GSH depletion and/or saturation of GSH conjugation may occur at lower dose levels for SEN than for SENO. At high dose levels this will thus lead to relatively higher pyrrole-protein adduct formation upon dosing SEN than upon dosing an equimolar dose of SENO, thereby resulting in a lower REP value when this REP value is calculated based on the ratio of $AUC_{pyrrole\text{-}protein}$ than when it is calculated based on the ratio of AUC_{SEN}. At lower dose levels, depletion of internal GSH and/or saturation of GSH conjugation will not occur and the REP value calculated based on the ratio of $AUC_{pyrrole\text{-}protein}$ will remain comparable to the REP value calculated based on the ratio of AUC_{SEN}. This result reveals that REP values should be quantified at realistic low dose levels. However, this will also obviously hamper their quantification in in vivo animal experiments, where generally high dose levels need to be applied to reach the relevant detection limits for the compounds and biomarkers under study.

In agreement to the statement of "all models are wrong, but some are useful,"[92] the model in the present study can be

considered as a useful first approximation to describe the respective kinetics. Our initial aim is to keep the model as simple as possible with parameters that can be obtained by either in vitro or in silico models. However, further refinements of the PBK model could be considered taking the following limitations of the model into account. 1) First of all, the model included aerobic liver metabolism of SENO, while some parts of the liver might be anaerobic, which, as also shown by our results, may result in more efficient reduction and higher REP values. 2) The model did not consider potential metabolism of SEN itself by the gut microbiota, also because in anaerobic fecal incubations with SEN there was no substantial degradation of SEN during the time frame of the incubations. In the present model, all SEN is assumed to be absorbed directly from the microbiota compartment to the liver. 3) More refined scaling from the in vitro to the in vivo situation of the rat microbiota kinetic parameters may be considered using microbial abundances and actual volumes of the respective gut microbial compartments; one might even consider to use intestinal content instead of fecal samples for the incubations, but this would significantly hamper the development of a human model. 4) Furthermore, it is of interest to note that the REP value seems to depend on the endpoint used: using the data from the in vivo rat study on SEN and SENO reported by Yang et al.,[11] it follows that the REP value calculated based on the $AUC_{pyrrole\text{-}protein}$ is lower than that calculated based on the AUC_{SEN}. The model enables quantification of the REP based on the AUC_{PA} and building an extended model that also allow prediction of the REP value based on the $AUC_{pyrrole\text{-}protein}$ would be of interest for further studies. This will require determination of the rate constants for GSH pyrrole-adduct formation and/or the potential dose dependent reduction of cellular GSH levels due to scavenging of the reactive pyrrole intermediates. 5) The model did not consider the reversible nature of the PA-N-oxide reduction given that PAs can be converted back to PA-N-oxides in the liver. However, it included PA conversion to PA-N-oxide as part of the clearance of the PA since that is known to include PA N-oxidation. 6) Potential transport from the intestinal cells back into the intestinal lumen was not taken into account, which may lead to decreased permeability of the intestinal wall and reduced bioavailability.[93] Reduced bioavailability as shown in an in vivo study[46,94] was however included in the model. 7) Furthermore, the PA retrorsine and its liver-derived reactive metabolites were reported to be transported by bile into the intestine to exert enterotoxicity, and the current model did not consider this aspect of the gut-liver axis.[21] 8) Finally, the role of additional liver microsomal enzymes in PA reduction other than CYPs is worth further investigation. Given the fact that the rate constant for liver S9 reduction of SENO obtained in microsomal incubations with NADPH regeneration system was higher than that obtained with NADPH, but did not provide better PBK model based predictions, warrants further investigations of these pathways and their in vivo relevance. All in all, in spite of these limitations, the PBK model did provide adequate predictions with only a limited number of kinetic parameters.

In conclusion, the present study demonstrates a novel proof of principle for use of a NAM based on in vitro and in silico data only to define in vivo REP values for PA-N-oxides. The results obtained confirm that these REP values are dose-dependent and higher at more realistic low dose levels than at the higher dose levels generally applied in in vivo studies in experimental animals, and also enable definition of REP values for human at realistic dietary exposure levels. Altogether, it is concluded that PBK modeling serves as valuable QIVIVE tool for predicting REP values of PA-N-oxides and may actually result in more accurate REP values for human risk assessment than what would be defined using in vivo animal experiments.

Supporting Information

Supporting Information is available from the Wiley Online Library or from the author.

Acknowledgements

Y.A. received a scholarship for his PhD studies at Wageningen University from Qassim University with grant number 35796. J.Y. received a scholarship for her M.Sc. studies at Wageningen University from Bhutan Agriculture and Food Regulatory Authority with financial assistance from the Dutch government (grant number OKP-MA.20/02042). The Data Availability Statement was added on February 20, 2023.

Conflict of Interest

The authors declare no conflict of interest.

Author Contributions

I.M.C.M.R. designed the scope of the manuscript. F.W., Y.A., J.Y., and S.W. performed experiments and interpreted data. F.W. and I.M.C.M.R. developed the PBK model. F.W. wrote the manuscript and Y.A., J.Y., S.W., and I.M.C.M.R. reviewed and edited the manuscript. All authors read and approved the final manuscript.

Data Availability Statement

The data that support the findings of this study are available from the corresponding author upon reasonable request.

Keywords

human, physiologically based kinetic (PBK) model, rat, relative potency (REP) value, SEN, SENO

Received: May 6, 2022
Revised: October 30, 2022
Published online: January 24, 2023

[1] L. Smith, C. Culvenor, *J. Nat. Prod.* **1981**, *44*, 129.
[2] O. Mohabbat, M. S. Younos, A. Merzad, R. Srivastava, G. G. Sediq, G. N. Arama, *Lancet* **1976**, *308*, 269.
[3] WHO-IPCS, *Environmental Health Criteria 80*, WHO, Geneva, **1988**, pp. 1-345.
[4] EFSA, J. Alexander, L. Barregård, M. Bignami, B. Brüschweiler, S. Ceccatelli, B. Cottrill, M. Dinovi, L. Edler, B. Grasl-Kraupp, C. Hogstrand, L. R. Hoogenboom, H. K. Knutsen, C. S. Nebbia, I. P. Oswald, A. Petersen, M. Rose, A.-C. Roudot, T. Schwerdtle, C. Vleminckx, G. Vollmer, H. Wallace, *EFSA J* **2017**, *15*, e04908.

[5] R. J. Huxtable, *Perspect Biol Med* **1980**, *24*, 1.
[6] J. M. Watt, M. G. Breyer-Brandwijk, *The Medicinal and Poisonous Plants of Southern and Eastern Africa: Being an Account of their Medicinal and other Uses, Chemical Composition, Pharmacological Effects and Toxicology in Man and Animal*, E. & S. Livingstone, Edinburgh, UK **1962**.
[7] T. Hartmann, G. Toppel, *Phytochemistry* **1987**, *26*, 1639.
[8] A. E. Johnson, R. J. Molyneux, G. B. Merrill, *J. Agric. Food Chem.* **1985**, *33*, 50.
[9] H. Sander, T. Hartmann, *Plant Cell Tissue Organ Cult.* **1989**, *18*, 19.
[10] Z.-B. Tu, C. Konno, D. D. Soejarto, D. P. Waller, A S. Bingel, R. J. Molyneux, J. A. Edgar, G. A. Cordell, H. H. S. Fong, *J. Pharm. Sci.* **1988**, *77*, 461.
[11] M. Yang, J. Ruan, H. Gao, N. Li, J. Ma, J. Xue, Y. Ye, P P.-C. Fu, J. Wang, Ge Lin, *Arch. Toxicol.* **2017**, *91*, 3913.
[12] B. L. Stegelmeier, J. A. Edgar, S. M. Colegate, D. R., Gardner, T. K. Schoch, R. A. Coulombe, R. J. Molyneux, *J. Nat. Toxins* **1999**, *8*, 95.
[13] Y. Cao, S. M. Colegate, J. A. Edgar, *Phytochem. Anal.* **2008**, *19*, 526.
[14] R. Molyneux, D. Gardner, S. Colegate, J. Edgar, *Food Addit. Contam. Part A* **2011**, *28*, 293.
[15] A. Mattocks, *Chemistry and Toxicology of Pyrrolizidine Alkaloids*, Academic Press, London **1986**.
[16] F. Widjaja, S. Wesseling, I. M. C. M. Rietjens, *Arch. Toxicol.* **2022**, *96*, 135.
[17] M. Yang, J. Ma, J. Ruan, Y. Ye, P P.-C. Fu, G. Lin, *Arch. Toxicol.* **2019**, *93*, 2197.
[18] A. R. Mattocks, *Xenobiotica* **1971**, *1*, 563.
[19] M. W. Chou, Y.-P. Wang, J. Yan, Y.-C. Yang, R. D. Beger, L. D. Williams, D. R. Doerge, P. P. Fu, *Toxicol. Lett.* **2003**, *145*, 239.
[20] Y.-P. Wang, J. Yan, P. P. Fu, M. W. Chou, *Toxicol. Lett.* **2005**, *155*, 411.
[21] Y. He, L. Zhu, J. Ma, G. Lin, *Arch. Toxicol.* **2021**, *95*, 1917.
[22] Y.-Q. He, L. Yang, H.-X. Liu, J.-W. Zhang, Y. Liu, A. Fong, A.-Z. Xiong, Y.-L. Lu, L. Yang, C.-H. Wang, Z.-T. Wang, *Chem. Res. Toxicol.* **2010**, *23*, 591.
[23] P. P. Fu, Q. Xia, G. Lin, M. W. Chou, *Drug Metab Rev* **2004**, *36*, 1.
[24] A. Mattocks, I. Bird, *Chem. Biol. Interact.* **1983**, *43*, 209.
[25] G. Lin, Y.-Y. Cui, E. M. Hawes, *Drug Metab. Dispos.* **1998**, *26*, 181.
[26] C. E. Green, H. Segall, J. L. Byard, *Toxicol. Appl. Pharmacol.* **1981**, *60*, 176.
[27] J. Ma, Q. Xia, P. P. Fu, G. Lin, *J. Food Drug Anal.* **2018**, *26*, 965.
[28] Q. Xia, Y. Zhao, L. S. Von Tungeln, D. R. Doerge, Ge Lin, L. Cai, P P. Fu, *Chem. Res. Toxicol.* **2013**, *26*, 1384.
[29] Q. Xia, X. He, L. Ma, S. Chen, P. P. Fu, *Chem. Res. Toxicol.* **2018**, *31*, 619.
[30] A. Allemang, C. Mahony, C. Lester, S. Pfuhler, *Food Chem. Toxicol.* **2018**, *121*, 72.
[31] J. Louisse, D. Rijkers, G. Stoopen, W. J. Holleboom, M. Delagrange, E. Molthof, P. P. J. Mulder, R. L. A. P. Hoogenboom, M. Audebert, A. A. C. M. Peijnenburg, *Food Chem. Toxicol.* **2019**, *131*, 110532.
[32] K.-H. Merz, D. Schrenk, *Toxicol. Lett.* **2016**, *263*, 44.
[33] F. Widjaja, Y. Alhejji, I. M. C. M. Rietjens, *Planta Med.* **2022**, *88*, 130.
[34] I. Geburek, D. Schrenk, A. These, *Arch. Toxicol.* **2020**, *94*, 3759.
[35] Y.-Q. He, Y. Liu, B.-F. Zhang, H.-X. Liu, Y. L. Lu, L. Yang, A. Z. Xiong, L. L. Xu, C. H. Wang, L. Yang, Z. T. Wang, *Drug Metab. Dispos.* **2010**, *38*, 626.
[36] D. M. Mendez-Catala, A. Spenkelink, I. M. C. M. Rietjens, K. Beekmann, *Toxicol. Rep.* **2020**, *7*, 938.
[37] Q. Wang, B. Spenkelink, R. Boonpawa, I. M. C. M. Rietjens, K. Beekmann, *Mol. Nutr. Food Res.* **2020**, *64*, 1900912.
[38] L. Chen, J. Ning, J. Louisse, S. Wesseling, I. M. C. M. Rietjens, *Food Chem. Toxicol.* **2018**, *116*, 216.
[39] J. Ning, L. Chen, M. Strikwold, J. Louisse, S. Wesseling, I. M. C. M. Rietjens, *Arch. Toxicol.* **2019**, *93*, 801.
[40] R. P. Brown, M. D. Delp, S. L. Lindstedt, L. R. Rhomberg, R. P. Beliles, *Toxicol. Ind. Health* **1997**, *13*, 407.
[41] A. Punt, N. Pinckaers, A. Peijnenburg, J. Louisse, *Chem. Res. Toxicol.* **2020**, *34*, 460.
[42] L. M. Berezhkovskiy, *J. Pharm. Sci.* **2004**, *93*, 1628.
[43] T. Cheng, Y. Zhao, X. Li, F. Lin, Y. Xu, X. Zhang, Y. Li, R. Wang, L. Lai, *J. Chem. Inf. Model.* **2007**, *47*, 2140.
[44] H. E. Cubitt, J. B. Houston, A. Galetin, *Pharm. Res.* **2009**, *26*, 1073.
[45] J. Lüthy, T. Heim, C. Schlatter, *Toxicol. Lett.* **1983**, *17*, 283.
[46] C. Wang, Y. Li, J. Gao, Y. He, A. Xiong, L. Yang, *Anal. Bioanal. Chem.* **2011**, *401*, 275.
[47] Y. Guo, H. Lee, H. Jeong, *Prog. Mol. Biol. Transl. Sci.* **2020**, *171*, 61.
[48] M. Yang, J. Ma, J. Ruan, C. Zhang, Y. Ye, P. P.-C. Fu, *J. Ethnopharmacol.* **2020**, *249*, 112421.
[49] J. Tang, Z. Wang, T. Akao, M. Hattori, *Asian J. Chem.* **2013**, *25*, 2027.
[50] T. Hartmann, C. Theuring, J. Schmidt, M. Rahier, J. M. Pasteels, *J. Insect Physiol.* **1999**, *45*, 1085.
[51] R. Swick, P. Cheeke, N. Patton, D. Buhler, *J. Anim. Sci.* **1982**, *55*, 1417.
[52] J. Brauchli, J. Lüthy, U. Zweifel, C. Schlatter, *Exp. Suppl.* **1982**, *38*, 1085.
[53] G. Powis, M. M. Ames, J. S. Kovach, *Cancer Res.* **1979**, *39*, 3564.
[54] R. Lindigkeit, A. Biller, M. Buch, H. M. Schiebel, M. Boppré, T. Hartmann, *Eur. J. Biochem.* **1997**, *245*, 626.
[55] D.-S. Yim, S. Choi, S. H. Bae, *Transl. Clin. Pharmacol.* **2020**, *28*, 126.
[56] T. Kimura, K. Higaki, *Biol. Pharm. Bull.* **2002**, *25*, 149.
[57] L. C. Hoskins, N. Zamcheck, *Gastroenterology* **1968**, *54*, 210.
[58] D. M. Mendez-Catala, Q. Wang, I. M. C. M. Rietjens, *Mol. Nutr. Food Res.* **2021**, *65*, 2100443.
[59] C. Rose, A. Parker, B. Jefferson, E. Cartmell, *Crit. Rev. Env. Sci. Technol.* **2015**, *45*, 1827.
[60] C. Behr, S. Sperber, X. Jiang, V. Strauss, H. Kamp, T. Walk, M. Herold, K. Beekmann, I. M. C. M. Rietjens, B. van Ravenzwaay, *Toxicol. Appl. Pharmacol.* **2018**, *355*, 198.
[61] Q. Wang, B. Spenkelink, R. Boonpawa, I. M. C. M. Rietjens, *J. Agric. Food Chem.* **2021**, *70*, 343.
[62] A., Punt, A. P., Freidig, T., Delatour, G., Scholz, M. G. Boersma, B. Schilter, P. J. van Bladeren, I. M. C. M. Rietjens, *Toxicol. Appl. Pharmacol.* **2008**, *231*, 248.
[63] H. E. Cubitt, J. B. Houston, A. Galetin, *Drug Metab. Dispos.* **2011**, *39*, 864.
[64] K. Walton, J. Dorne, A. Renwick, *Food Chem. Toxicol.* **2004**, *42*, 261.
[65] A. Noorlander, S. Wesseling, I. M. C. M. Rietjens, B. van Ravenzwaay,, *Toxicol. Lett.* **2021**, *343*, 34.
[66] M. Lobell, V. Sivarajah, *Mol. Divers* **2003**, *7*, 69.
[67] J. Ebmeyer, J. D. Rasinger, J. G. Hengstler, D. Schaudien, O. Creutzenberg, A. Lampen, A. Braeuning, S. Hessel-Pras, *Arch. Toxicol.* **2020**, *94*, 1739.
[68] R. Schoental, P. N. Magee, *J. Pathol. Bacteriol.* **1959**, *78*, 471.
[69] EFSA, *EFSA J.* **2011**, *9*, 2406.
[70] M. V. Evans, M. E. Andersen, *Toxicol. Sci.* **2000**, *54*, 71.
[71] H. Nishimuta, T. Nakagawa, N. Nomura, M. Yabuki, *Xenobiotica* **2013**, *43*, 948.
[72] I. Geburek, A. Preiss-Weigert, M. Lahrssen-Wiederholt, D. Schrenk, A. These, *Food Chem. Toxicol.* **2020**, *135*, 110868.
[73] J. T. Hovermale, A. M. Craig, *Biophys. Chem.* **2002**, *101*, 387.
[74] A. T. Dick, A. Dann, L. Bull, C. Culvenok, *Nature* **1963**, *197*, 207.
[75] A. Mattocks, *Nature* **1968**, *217*, 723.
[76] C. S. Mazur, J. F. Kenneke, M.-R. Goldsmith, C. Brown, *Drug Metab. Dispos.* **2009**, *37*, 1801.
[77] K. Lavrijsen, D. Van Dyck, J. Van Houdt, J. Hendrickx, J. Monbaliu, R. Woestenborghs, W. Meuldermans, J. Heykants, *Drug Metab. Dispos.* **1995**, *23*, 354.
[78] H. Mönnikes, B. G. Schmidt, Y. Taché, *Gastroenterology* **1993**, *104*, 716.
[79] L. Degen, S. Phillips, *Gut* **1996**, *39*, 299.
[80] J. Koopman, M. Van den Brink, R. Smits, *Microb. Ecol. Health Dis.* **1989**, *2*, 279.

[81] L. Skálová, U. Nobilis, B. Szotáková, V. Wsól, E. Kvasnieková, *Drug Metabol. Drug Interact* **1998**, *14*, 235.
[82] F. Kolrep, J. Numata, C. Kneuer, A. Preiss-Weigert, M. Lahrssen-Wiederholt, D. Schrenk, A. These, *Arch. Toxicol.* **2018**, *92*, 1089.
[83] C. L. Miranda, R. L. Reed, F. P. Guengerich, D. R. Buhler, *Carcinogenesis* **1991**, *12*, 515.
[84] R. Vuppalanchi, *Practical Hepatic Pathology: A Diagnostic Approach E-Book: A Volume in the Pattern Recognition Series*, Elsevier, Philadephia, PA **2011**, p. 45.
[85] Y. Kamiya, T. Miura, A. Kato, N. Murayama, M. Shimizu, H. Yamazaki, *Drug Metab. Lett.* **2021**, *15*, 64.
[86] J. A. Edgar, R. J. Molyneux, S. M. Colegate, *Chem. Res. Toxicol.* **2015**, *28*, 4.
[87] Q. Xia, Y. Zhao, G. Lin, F. A. Beland, L. Cai, P. P. Fu, *Chem. Res. Toxicol.* **2016**, *29*, 1282.
[88] M. Yang, J. Ruan, P. P. Fu, G. Lin, *Chem. Biol. Interact.* **2016**, *243*, 119.
[89] C. C. Yan, R. J. Huxtable, *Biochem. Pharmacol.* **1996**, *51*, 375.
[90] Y. Chen, L. Ji, H. Wang, Z. Wang, *Environ. Toxicol. Pharmacol.* **2009**, *28*, 357.
[91] X. Wang, G. C. Kanel, L. D. DeLeve, *Hepatology* **2000**, *31*, 428.
[92] G. Box, *Robustness Stat.* **1979**, *202*, 549.
[93] S. Suparmi, S. Wesseling, I. M. C. M. Rietjens, *Arch. Toxicol.* **2020**, *94*, 3281.
[94] A. Xiong, Y. Li, L. Yang, J. Gao, Y. He, C. Wang, Z. Wang, *J. Pharm. Biomed. Anal.* **2009**, *50*, 1070.